fibers

MDPI

Article

Performance of Fiber-Reinforced Ultra-High-Performance Concrete Incorporated with Microencapsulated Phase Change Materials

Mahmoud Rady and Ahmed M. Soliman *

Department of Building, Civil and Environmental Engineering, Concordia University, Montreal, QC H3G 1M8, Canada
* Correspondence: ahmed.soliman@concordia.ca

Abstract: In the era of environmental concerns, many attempts were proposed to optimize energy efficiency for buildings and consequently reduce their carbon footprint. As a sustainable approach, it is a promising solution to incorporate phase change materials (PCMs) in construction materials (i.e., ultra-high-performance concrete (UHPC)) to increase its thermal storage capacity and reduce the operation energy. However, incorporating microencapsulated phase change materials (MPCMs) into cementitious materials negatively impacts the fresh and hardened properties. UHPC's improved mechanical strength allows for the creation of slimmer and lighter structures, which may result in less demand in concrete manufacturing and fewer emissions. Hence, the properties of UHPC incorporated with MPCMs (MPCM-UHPC) need more investigations. To fill the gap in the literature about the lack of information about MPCM-UHPC performance, this paper provides a comprehensive work to study the mechanical, thermal, and impact resistance properties of (MPCM-UHPC). Proportions of 5% and 10% of MPCMs were incorporated as a replacement of sand by volume. Proportions of 0.5%, 1.0%, and 1.5% of micro steel fiber reinforcement were used as a percentage of the mixture's total volume. The results revealed the importance of fiber reinforcement in compensating for the negative effect of MPCMs inclusion for improving the thermal properties. Increasing the amount of MPCMs enhanced the thermal performance of the produced UHPC panels through the ability to absorb and release the energy during the phase change process.

Keywords: ultra-high-performance concrete; microencapsulated phase change material; micro steel fiber; thermal performance; modified Charpy impact

Citation: Rady, M.; Soliman, A.M. Performance of Fiber-Reinforced Ultra-High-Performance Concrete Incorporated with Microencapsulated Phase Change Materials. *Fibers* **2023**, *11*, 94. https://doi.org/10.3390/fib11110094

Academic Editor: Messaoud Saidani

Received: 1 September 2023
Revised: 25 October 2023
Accepted: 30 October 2023
Published: 3 November 2023

1. Introduction

Buildings are now the world's greatest energy consumers due to population expansion and an increased reliance on cooling and heating systems [1]. The potential to reduce the annual cooling and heating demand by up to 50% has been demonstrated by using phase change material (PCM) [2,3]. Currently, the direct inclusion of PCM into cement-based materials is creating a significant debate in the scientific community over the wise choice and effective application of PCM [2]. PCMs are the materials used to store latent heat energy and have the ability to absorb or release thermal energy through temperature changes under controlled circumstances [4,5]. The main benefits of PCMs, which enable them to be successfully applied in buildings for thermal management, are their singular and high storage capacity with small temperature fluctuations due to the phase transition of PCMs at the melting point and typically minor volume changes [6,7]. As a result, PCMs have been recognized as one of the most progressive materials to enhance energy efficiency and sustainability in buildings, especially for heating and cooling [8–10].

In recent years, researchers have conducted many studies to assess the thermal performance of building materials containing phase change materials (PCMs). These materials can be integrated into various building components, such as wallboards [11,12], roofs and

ceilings [13], floors [14,15], external walls [16], windows [17,18], bricks [19,20], mortars and concrete [21–23]. Changes in concrete, the most commonly used construction material, characteristics were assessed after PCM inclusion in various formats, including microcapsules, porous lightweight aggregates loaded with PCMs, and shape-stabilized PCMs (SSPCMs) [24,25]. Incorporating microencapsulated PCMs (MPCMs) in concrete is the most popular method [26,27]. The microencapsulation technique is defined as the process by which one or more compounds in the form of discrete solid particles or liquid droplets (e.g., the core) are encased in a protective layer using a continuous polymeric film made of one or more materials (e.g., the shell); or by which the internal core material is dispersed throughout the shell, primarily to separate the core ingredient (PCM) from the environment and protect it as a result [28]. Most MPCMs are produced as powders with adequate morphological and size properties. MPCMs are typically added to concrete or mortar as a partial replacement for fine particles [2]. Although utilizing MPCMs increases the thermal inertia of concrete by increasing its thermal energy storage capability, it drastically degrades its mechanical properties [26]. Numerous researchers have extensively highlighted concerns about the potential leaking of PCM paraffin in the liquid state [20,29–31], and microcapsule rupture during mixing or under loads [30,32–36].

To mitigate the negative effects of MPCMs in cementitious materials, enhancing the properties by using excellent properties of cement composites can be a vital solution (i.e., UHPC). Compared with ordinary concrete, UHPC is a new type of sustainable and environmentally friendly material with high compressive strength, tensile ductility, and toughness [37,38]. Reactive powders and fibers are typically added to the mixture to meet design requirements. Reactive powders can fill the fine pores, producing an extremely dense material structure [39–42]. Micro steel fibers boost the mixture's ability to withstand flexural and tensile loads after initial cracking, resulting in higher toughness. Applications of UHPC will undoubtedly encourage "do more with less" and "build to last," leading to a significant reduction in the amount of CO_2 embodied in concrete [43].

Generally, to our knowledge, the properties of MPCM-UHPC have not been highlighted in prior research except in the previous study by Ren et al. [44]. Ren et al. studied the effect of adding MPCMs as a percentage of the binder's mass on the UHPC's properties reinforced by a constant percentage of micro steel fiber 1%, including thermal performance, mechanical properties, and shrinkage strain. The previous study adopted adding MPCMs as a percentage of the mass of the binder. However, the incorporation of MPCMs as a replacement for sand volume was reported to produce better performance for cementitious materials [35]. The previous study did not cover the effect of changing fiber percentages on the properties and the combined effect of MPCM incorporation.

Hence, this study aims to expand upon previous research by exploring the impact of varying percentages of micro steel fiber and MPCMs (as replacement of sand volume) on the properties of UHPC. Moreover, a modified Charpy impact test was applied to determine the effect of these factors on the dynamic properties. This research is anticipated to advance knowledge of the properties of MPCM-UHPC and its potential applications in various industries.

2. Materials and Methods

2.1. Materials

General-used (GU) hydraulic cement according to the CSA-3001-03 (Cementitious Materials for Use in Concrete) (CSA, 2013) [45], silica fume (SF) complies with ASTM C1240-05 [46], and Class F fly ash (FA) ASTM C618 [47] were used as cementitious materials for all tested UHPC. Physical features and chemical compositions for GU, SF and FA are summarized in Table 1. Natural riverside sand with a fineness modulus, specific gravity, and water absorption of 2.70, 2.51, and 2.73% was used as the main aggregate. The aggregate was in a saturated surface dry condition. A commercial MPCM with a paraffin wax core encased with a melamine shell (Figure 1) and was added as a volume replacement of sand. Thermo-physical characteristics of the MPCMs are summarized in

Table 2. Copper-coated micro steel fiber with a yield strength of 2850 MPa, specific gravity of 7.85, a diameter of 0.2 ± 0.02 mm and length of 14 ± 1 mm, as shown in Figure 2, was added at rates 0.5%, 1.0% and 1.5% to improve the mechanical properties, by total volume. A high-range-water-reducer (HRWR) polycarboxylate ether-based admixture adjusted the workability.

Table 1. Chemical and physical properties of general-used cement, fly ash and silica fume.

Item	GU	FA	SF
SiO_2	19.80%	43.39	96.00
Al_2O_3	4.90%	22.08	1.10
CaO	62.30%	15.63	1.20
Fe_2O_3	2.30%	7.74	1.45
SO_3	3.70%	1.72	0.25
K_2O	0.83%	-	1.20
Na_2O	0.34%	1.01	0.45
MgO	2.80%	-	0.18
P_2O_5	0.11%	-	
Na_2Oeq	0.87%	-	
Loss on ignition	1.90%	0.58	
Specific gravity	3.15	2.50	2.20
Surface area (m^2/kg)	360	280	17.8×10^3

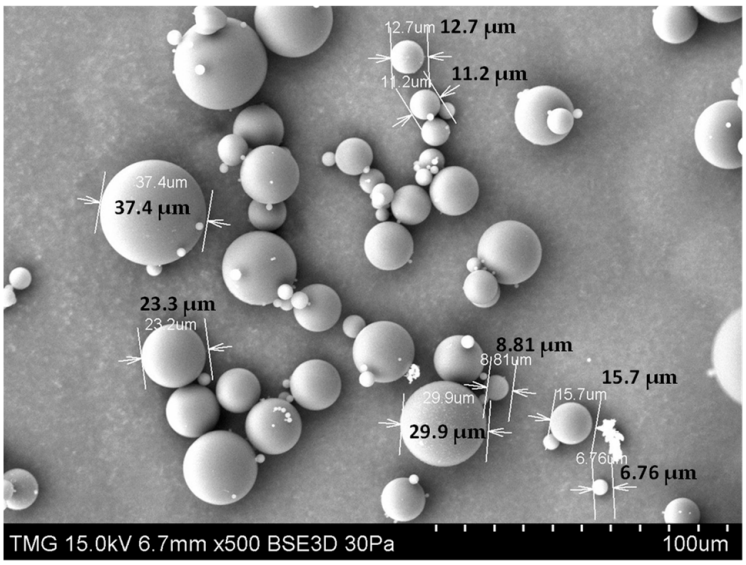

Figure 1. Micro-encapsulated phase change materials (SEM).

Table 2. Thermo-physical properties of MPCMs.

Properties	Values
Core	Paraffin wax
Shell Melamine	Formaldehyde (MF)
Tm, peak (°C)	24
Bulk Density (kg/cm^3)	~600
Latent Heat Capacity (J/g)	192
Mean particle size (µm)	15–30
Appearance	White Powder

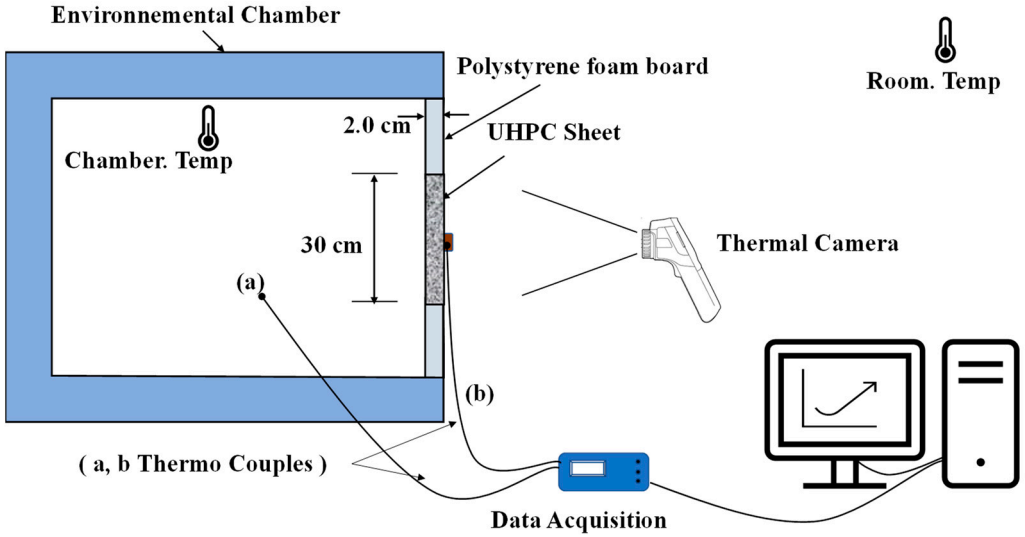

Figure 2. Thermal performance test setup.

2.2. Mixing Procedure

The mixture proportions including, cement, S.F, F.A, sand, water and HRWR as a ratio of cement weight are shown in Table 3. UHPC incorporated micro steel fiber of (0.5, 1.0, 1.5) % by volume of the mixture. MPCM of 5% and 10% was incorporated as a replacement of sand volume. For four minutes, cement, silica fume, and sand were mixed. Water and SP were added for an 8 min mixing phase. A homogeneous dispersion of micro steel fiber was achieved after another 8 min of mixing. Finally, MPCMs were gradually added for 1.5 min to reduce any damage to the shell. The specimens were demolded and maintained in a steam curing chamber at 90 °C for 72 h after undergoing conventional curing for 24 h [44,48].

Table 3. Mixture compositions.

Mix	Cement	SF	FA	Sand	HRWR	Water	MPCMs%	Micro Steel Fiber%
M1	1.0	0.23	0.18	1.27	0.04	0.29	0.0%	0.0%
M2								0.50%
M3								1.0%
M4								1.50%
M5	1.0	0.23	0.18	1.20	0.04	0.29	5.0%	0.0%
M6								0.50%
M7								1.0%
M8								1.50%
M9	1.0	0.23	0.18	1.14	0.04	0.29	10.0%	0.0%
M10								0.50%
M11								1.0%
M12								1.50%

2.3. Tests and Specimens Preparations

2.3.1. Characterization of MPCM-UHPC

The flowability of the designed mixtures was measured according to ASTM C1437-15 "Standard Test Method for Flow of Hydraulic Cement Mortar" [49], a mini-slump cone with a base diameter of 100 mm, a top diameter of 70 mm, and a height of 60 mm were used for the slump flow test. Accordingly, a mixture was poured into the cone and placed on a flat, levelled base. The slump cone was then raised upward. The maximum diameter and the diameter perpendicular to its phase were measured after the mortar flow was stopped. The result was based on the average value.

Cubic specimens 50 mm × 50 mm × 50 mm were used to evaluate the compressive strength at 28 days of curing according to ASTM C109/109 M "Standard Test Method for Compressive Strength of Hydraulic Cement Mortars (Using 2-in. or [50 mm] Cube Specimens)" [50].

To evaluate the flexural strength of UHPC specimens, a universal testing machine (UTM) was used to perform a three-point loading test with a span of 120 mm at a rate of 0.4 mm/min on (40 mm × 40 mm) area × 160 mm specimens at 28 days of curing according to ASTM-C348 "Standard Test Method for Flexural Strength of Hydraulic-Cement Mortars" [51]. The flexural strength can be calculated by Equation (1). All reported results represent the average of triplicate specimens.

$$Flexural\ strength = \frac{1.5P_{max}L}{B^3} \quad (1)$$

where:

P_{max}: The maximum load determined by the load-deflection curve.

L: The span.

B: The side length of the cross-section.

2.3.2. Thermal Performance Test of MPCM-UHPC Sheets

As shown in Figure 2, thermal performance was measured on 30 cm × 30 cm rectangular MPCM-UHPC panels with a thickness of 2.0 cm. The MPCM-UHPC panel was fitted in a polystyrene foam board, and then the polystyrene foam board with the UHPC panel was allowed to cool naturally for 24 h and then installed as a test room wall. The heat profile of the environmental chamber was adjusted to produce heat fluctuating around the melting point of the used MPCMs (i.e., 24 ± 2 °C). The temperature remained at the maximum temperature for one hour. Then, it returned to the start temperature, as shown in Figure 3. The temperature changes inside the environmental chamber and the corresponding temperature changes in the UHPC-MPCMs panels surfaces were recorded using thermocouples. Moreover, a high-resolution, forward-looking infrared (FLIR) camera, which converts thermal energy into visible light, was used to capture and monitor the changes in the outer surface temperature of the panels during the process.

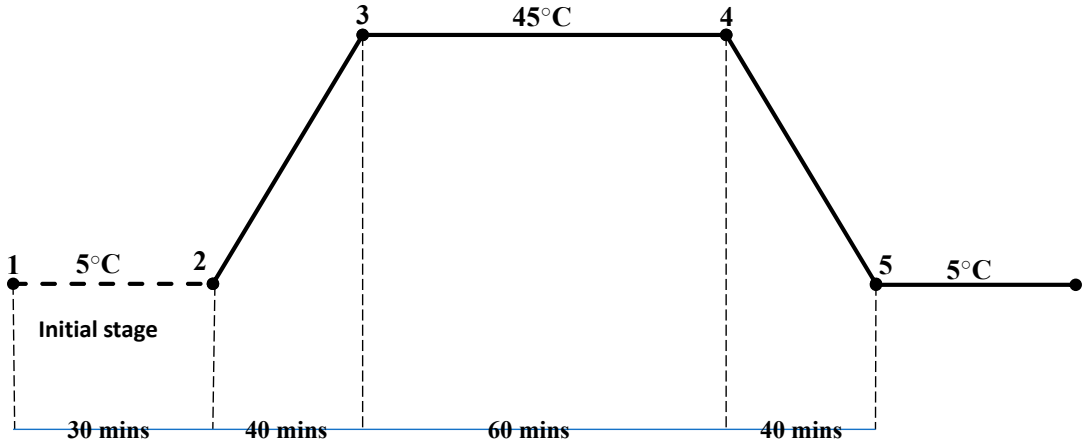

Figure 3. Heat profile adjusted for environmental chamber.

2.3.3. Impact Resistance

Based on the device created by Yu et al. [52], a downsized model of the "Modified Charpy Impact Device" was created. Using the modified Charpy impact test, two 340 × 40 × 20 mm^3 prisms from each mix were utilized to evaluate how much energy each mix design could absorb. These prisms were positioned in the hammer's circular path, reducing the hammer's energy. The 2.9 kg hammer and its holders were attached

to a pendulum that was released from height H_1 and swung to height H_2 after striking the specimen (Figure 4a,b). Following the energy conservation law, the modified Charpy impact test states that an object's total energy (the sum of its potential energy, kinetic energy, and energy loss) was constant. The impactor's total energy was equal to the potential energy due to the impactor's height when it was at H_1. The kinetic energy was at its highest, and the potential energy was zero when the specimen was first placed. The height of the hammer before and after the hit was used to calculate the energy lost by the specimen during the test. It should be emphasized that the results considered the machine's energy loss (without the specimen) to offset the energy lost during machine movement. According to the energy equilibrium relationship, the lowest height hammer's maximum contact velocity (V_c) to the specimen can be computed as follows (Equation (2)):

$$V_c = \sqrt{2g(H_1 - H_2)} \tag{2}$$

where g is the acceleration due to gravity (g = 9.806 m^2/s). The impactor is raised to the height of H_2 by the residual energy following the collision. The energy absorbed by the specimen is equal to the difference in total energy of the pendulum before and after the collision, according to Equations (3) and (4), assuming that friction on the device is low (less than 1% of the total impact energy)

$$U_1 + K_1 = U_2 + K_2 + W_c \tag{3}$$

$$W_c = M \times g \times (H_1 - H_2) \tag{4}$$

where U_1 and K_1 refer to the original pendulum's potential and kinetic energy, respectively. The final stage of the pendulum's potentials and kinetic energy are represented by U_2 and K_2, respectively. Additionally, M and W_c refer to the impactor's mass and the specimen's ability to dissipate energy, respectively.

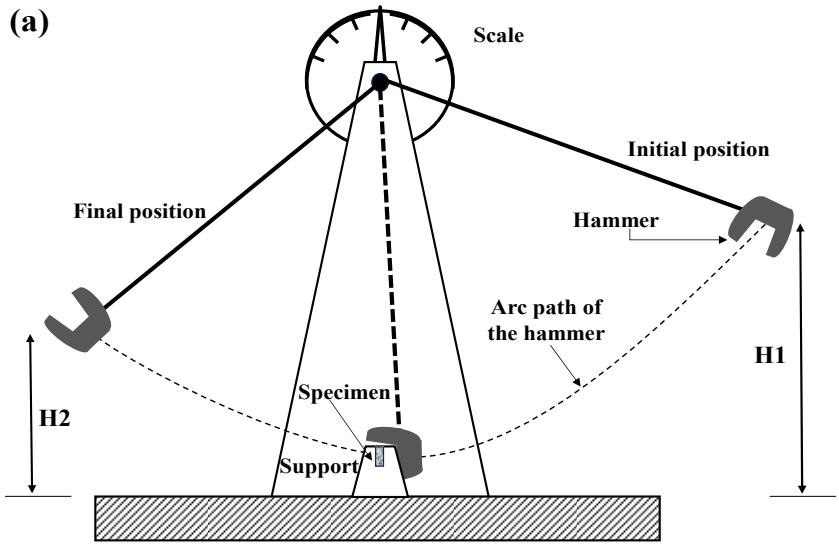

Figure 4. *Cont.*

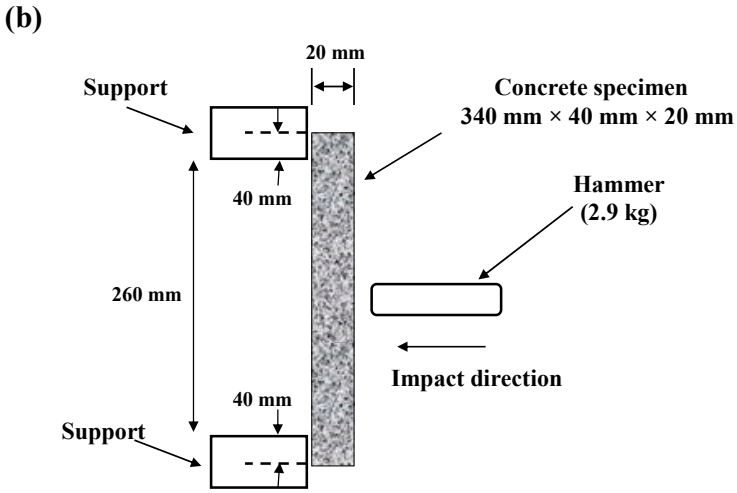

Figure 4. Modified Charpy impact (**a**) working scheme (**b**) modified setup.

3. Results and Discussion

3.1. Effects of MPCMs Content and Micro Steel Fiber Content on Flowability of UHPC

The effects of MPCMs and micro steel fiber content on the flowability of fresh UHPC mixtures are shown in Figure 5. The control batch (M1) had a flowability of 325 mm. The flowability seems to be unaffected by the increasing MPCM content in a verified range. For the inclusion of MPCMs of 5% and 10%, there was only about a +1% and −1% difference from the reference, respectively, as shown in Figure 5a. Due to the high flowability of UHPC, MPCMs have an insignificant effect on the workability of high-performance cementitious composites, which agreed with Hunger et al.'s [30] study on self-compacting concrete containing MPCMs. In contrast, for a constant amount of MPCMs, with the incorporation of 0.5%, 1%, and 1.5% micro steel fibers, the flowability linearly decreased by around 1.6%, 3.5%, and 5.2%, respectively, as shown in Figure 5b. This is attributed to the increase in the specific surface area associated with the increase in the fiber content [53]. Furthermore, the micro steel fibers were randomly distributed throughout the matrix and served as a skeleton, preventing fresh concrete flow [54].

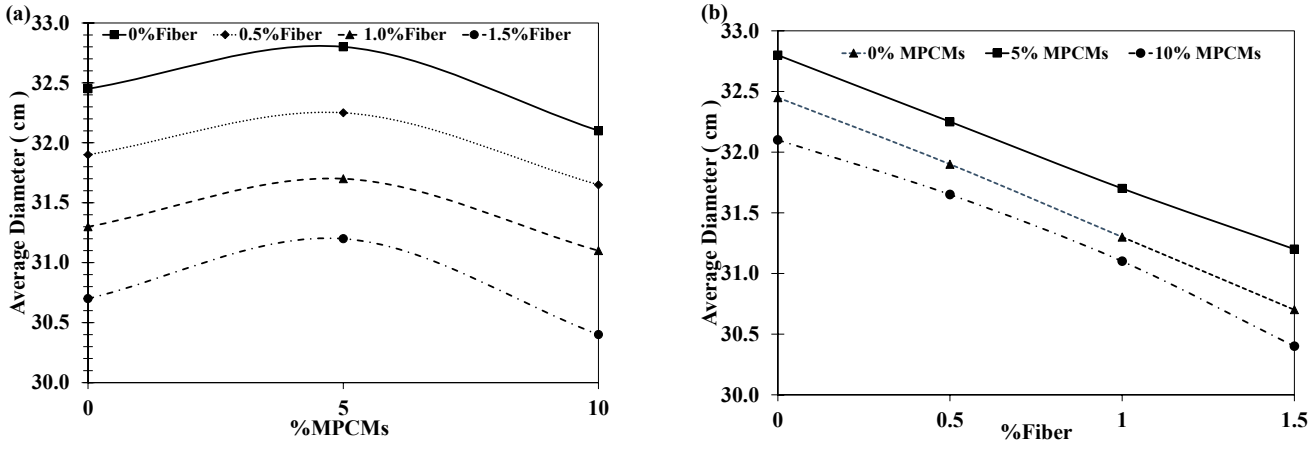

Figure 5. (**a**) Effect of increasing MPCMs content on flowability. (**b**) Effect of increasing fiber content on flowability.

3.2. Analysis of Strength Results

3.2.1. Compressive Strength

Figure 6 shows the 28-day compression strength for the various UHPC mixtures; adding micro steel fiber enhanced the strength. The compressive strength of UHPC increased gradually with the increase in fiber content. For instance, the strength was increased

by 5.7%, 10.0%, and 16.3% by adding 0.5%, 1.0%, and 1.5% fibers, respectively. The increase in compressive strength is caused by an increase in density and rigidity when micro steel fibers are present, as well as an improvement in the fibers' ability to control the spread of microcracks before they reach their maximum strength (Figure 7). This is following the results reported in references [55,56].

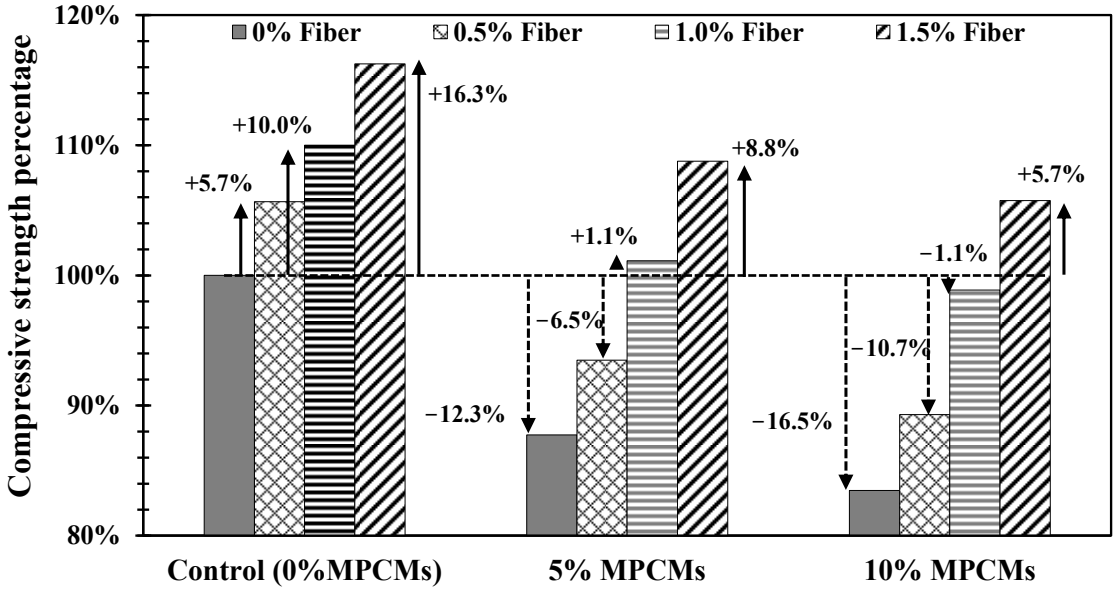

Figure 6. The 28 days Compressive Strength results as a percentage of the control mix result.

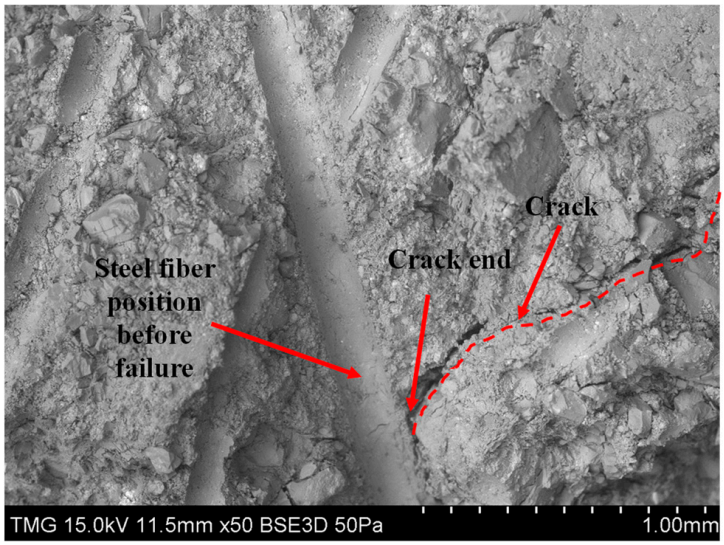

Figure 7. Micro steel fiber for preventing crack spread (SEM).

Conversely, the compressive strength decreased as the proportion of MPCMs in the mix increased. For instance, the compressive strength of mixtures containing 5% and 10% MPCMs decreased by 12.3% and 16.5% compared to that of the control; the microcapsules' low strength can explain this. The paraffin leakage caused by the shell breaking during mixing (Figure 8), the additional irregular void space, and the weak interface with the matrix are additional effects (Figure 9) [26,35,36,57,58].

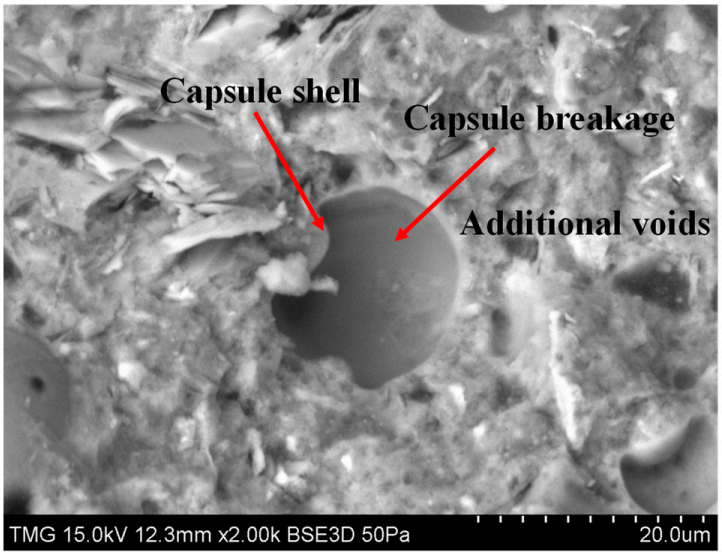

Figure 8. MPCM capsule breakage (SEM).

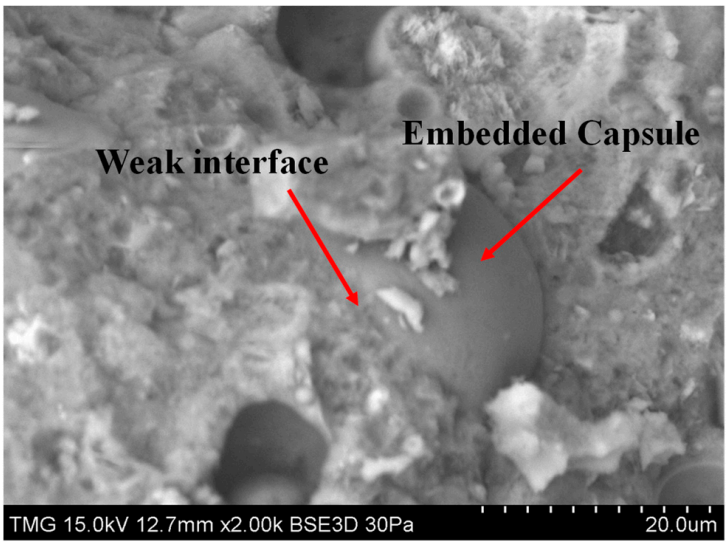

Figure 9. MPCM embedded capsule (SEM).

The results showed that adding micro steel fibers significantly compensated for the loss of compressive strength caused by the inclusion of MPCMs. This was attributed to the fact that the addition of fibers constrained the matrix materials around the particle at the micro-scale, creating a state of triaxial compression [59]. This mechanism significantly compensated for the strength loss caused by adding phase change material. The results revealed that adding $\geq$1.0% of micro steel fiber eliminates the reduction in the strength due to MPCMs incorporation while adding 0.5% fiber compensated for some of the strength loss. For instance, the strength was reduced by 16.5% by adding 10% of MPCMs (M9). However, the strength reduction was compensated by −10.70%, −1.10%, and +5.70% by adding 0.5%, 1.0% and 1.5% micro steel fibers, respectively (M10, M11, and M12).

3.2.2. Flexural Strength

Figure 10 shows the 28-day flexural strength results. Generally, the flexural strength gradually increased with the increase in micro steel fiber content. For instance, the flexural strength of the UHPC matrix with 0.5%, 1.0% and 1.5% micro steel fibers increased by approximately 7.3%, 43.8% and 55.2% compared to that of the control. This is attributed

to the ability of fiber to delay the initiation of micro-crack and to prevent crack propagation [60–63]. However, the incorporation of MPCMs negatively affected the flexural strength results. This was ascribed to the MPCM inclusions' excessive debonding, which causes lower fracture toughness (KIC) values with increasing MPCM volumes as well as composite weakening [64].

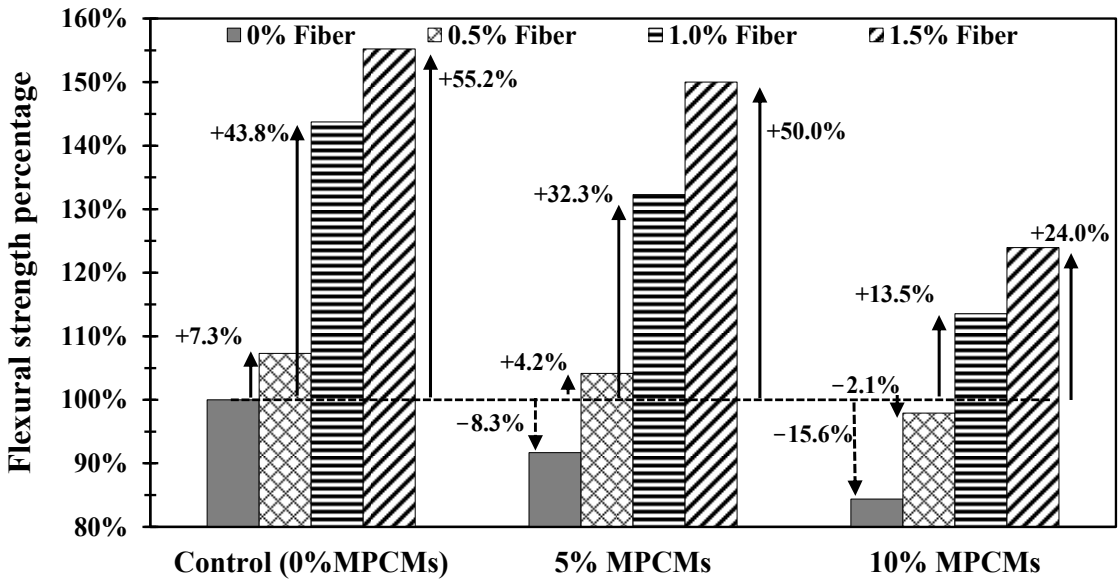

Figure 10. The 28-day Flexural Strength results as a percentage of the control mix result.

Figure 10 showed that the strength gained due to fiber reinforcement compensated for the loss due to MPCMs incorporation. Compared to the control mix (M1), adding ≥0.5% micro steel fiber overcomes the reduction in the strength due to MPCMs incorporation. For instance, for mixtures with 10% of MPCMs, the reduction in the strength was a 15.60% reduction (M9). However, adding 0.5%, 1.0% and 1.5% micro steel fibers (M10, M11, and M12, respectively) has successfully compensated for the strength reduction by −2.10%, +13.50%, and +24.0%, respectively.

3.2.3. Impact Resistance

Figure 11 depicts the impact testing of samples with and without adding micro steel fiber. The reinforced samples consistently revealed two parallel rectangle-like fractions, while the samples with 0% fiber exhibited four parallel rectangle-like fractions (Figure 11a). Furthermore, the concrete matrix was damaged following the impact loading, and all embedded micro steel fibers were pulled out at the fracture surfaces. Therefore, the energy absorption of the samples could be attributed to two main factors, including the energy consumed to break the concrete matrix and the energy spent to pull out the fibers from the damaged cross-sections (Figure 11b).

To quantify the energy dissipation capacity of concrete, the impact energy absorption of the mixtures was analyzed, as illustrated in Figure 12. The results indicated that the absorbed impact energy of the UHPC gradually increased as the fiber volume fraction increased. For instance, in the mixes group containing 0% MPCMs, the impact energy absorption of mixtures containing 0.5%, 1.0%, and 1.5% micro steel fibers increased by 204.8%, 236.0%, and 428.5% higher than the control. This can be attributed to the significant amount of energy absorbed during debonding, stretching, and pulling out of these fibers (Figure 11b) [65,66]. The randomly oriented fibers arrest a micro-cracking mechanism and limit the propagation of cracks. This leads to improved strength and ductility of the concrete (Figure 9) [65,66].

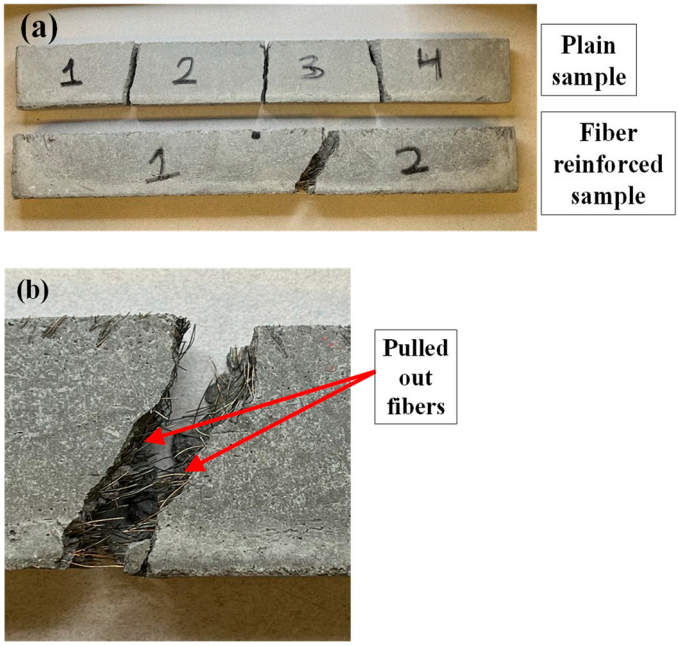

Figure 11. Fractions of the samples after impact test: (**a**) comparison of the reinforced and non-reinforced sample and (**b**) fractured surface of the reinforced sample and the pulled-out fibers.

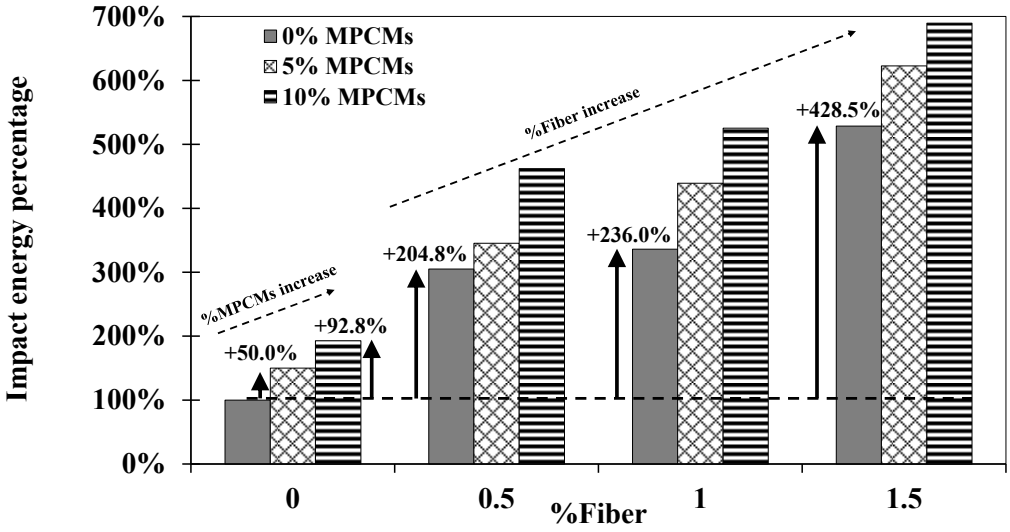

Figure 12. Variation of the absorbed impact energy of MPCM-UHPC with different short-fiber volume fractions and different %MPCMs.

Similarly, the absorbed energy increased as the proportion of MPCMs in the mix increased. For example, in the mix group containing 0% fiber, the absorbed energy of mixtures containing 5% and 10% MPCMs increased by 50.0% and 92.8% higher than the control. This behavior was attributed to the fact that the lower rigidity of MPCMs particles (Figure 13) decreased the modulus of elasticity of the matrix, resulting in greater elasticity and displacement under impact load. Furthermore, an increase in the amount of MPCM facilitated the production of a more heterogeneous composite, resulting in energy dissipation via rebounding or deforming rather than cracking [67].

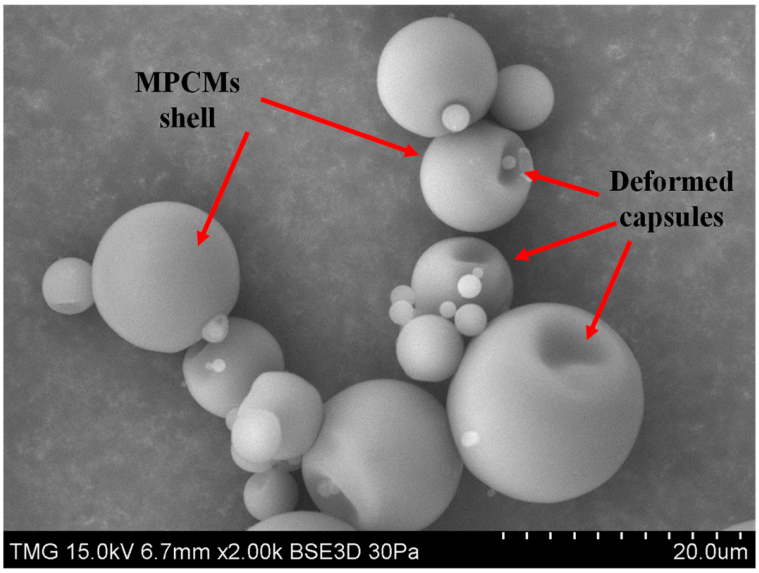

Figure 13. MPCM capsule deformation—low rigidity capsules (SEM).

3.2.4. Thermal Performance

Typical time-temperature profiles were recorded from the thermocouples located at the center of the sheets' outer and inner surfaces, as shown in Figure 14a,b.

MPCMs were employed to enhance the thermal performance of UHPC panels. As a result of this enhancement, the heating rate during the PCMs melting process decreased by increasing %MPCMs. For instance, the heating rate changed to be +0.52 °C/min and +0.37 °C/min by adding 5% MPCMs and 10% MPCMs, respectively. This change in heating rate was about 11.0% and 32.7%, respectively, lower than the rate of panels with 0% MPCMs (i.e., +0.56 °C/min) (Figure 14a).

Conversely, during the solidification, the cooling rate increased to −0.53 °C/min and −0.37 °C/min by adding 5% MPCMs and 10% MPCMs, respectively. This change in cooling rate was about 24.0% and 35.0%, respectively, higher than the rate of panels with 0% MPCMs with (i.e., −0.57 °C/min) (Figure 14a). These rates experienced a great change during the phase change process.

Steel has a thermal conductivity that is substantially higher than cement concrete at approximately 53 W/(mK). Theoretically, concrete with a higher percentage of steel fibers results in greater thermal conductivity. However, the addition of steel fibers and fiber agglomeration will increase the porosity of the concrete, particularly with higher steel fiber content, which significantly reduces thermal conductivity and offsets any increase in the thermal conductivity of the samples [43,68–72]. The thermal properties of the UHPC with different steel fiber contents are plotted in Figure 14b, where the MPCM content of the mixture is fixed at 0%. This study showed that adding steel fiber decreased thermal conductivity, especially with a higher %steel fiber (i.e., ≥0.5%). As shown in (Figure 14b), the addition of micro steel fiber lowers the rate of heat transfer through the sheets during the heating process, peak temperature, and cooling process. For instance, during the heating process, the rate changed to +0.49 °C/min, +0.42 °C/min and +0.39 °C/min by adding 0.5%, 1.0% and 1.5% of steel fiber, respectively.

Overall, the results showed that adding MPCMs and micro steel fiber decreases the thermal conductivity of the sheets and affects their thermal performance during heating and cooling processes. Additionally, MPCMs enhance the thermal energy efficiency of the panels by absorbing and releasing the heat during the phase change process. Moreover, adding micro steel fiber with UHPC panels incorporated with MPCMs will affect the overall thermal performance (decrease the thermal conductivity) in response to changes in temperature (Figure 14c).

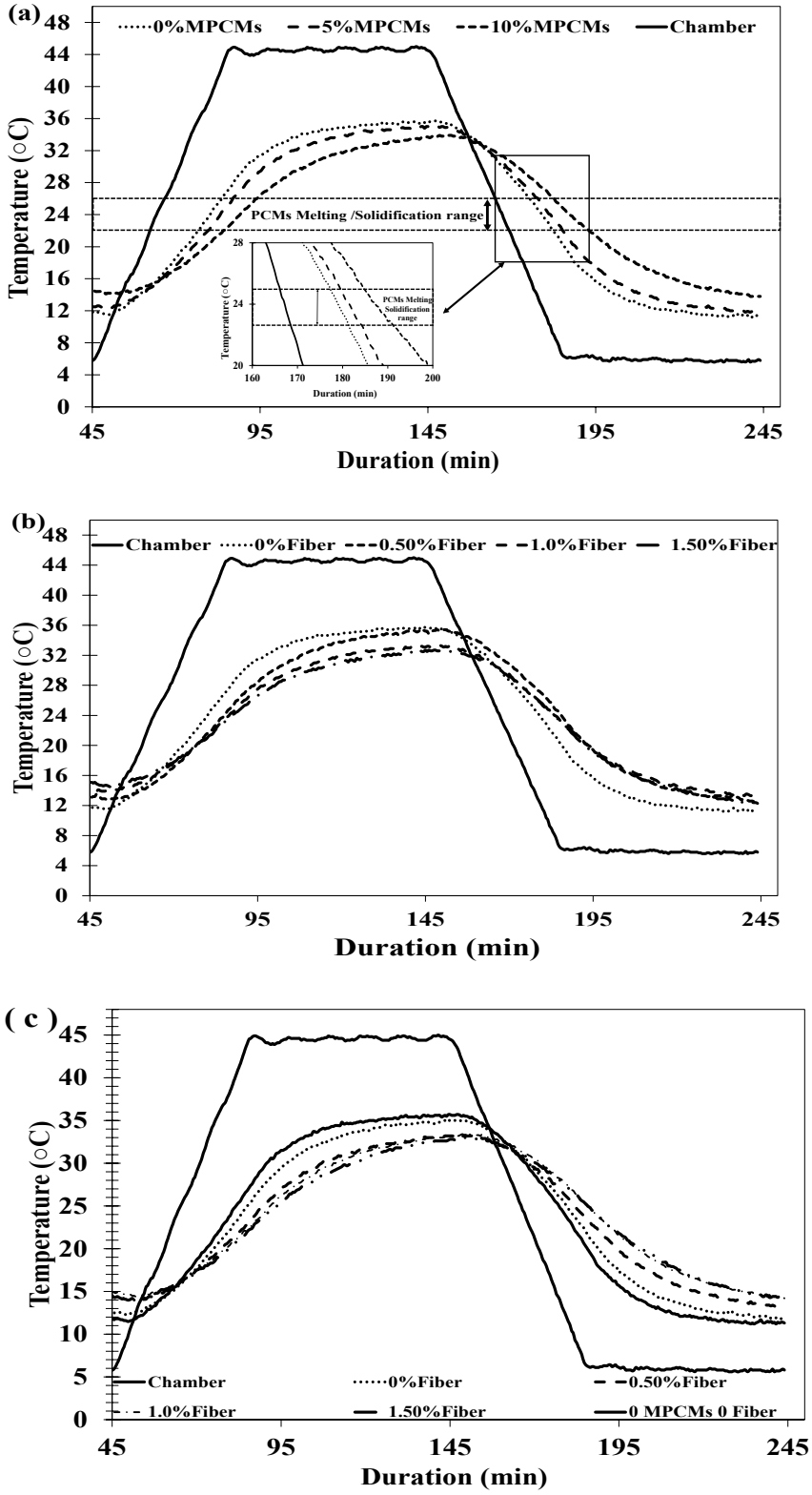

Figure 14. (**a**) Effect of increasing MPCM content on thermal performance. (**b**) Effect of increasing fiber content on thermal performance. (**c**) Combined effect of MPCMs and steel fiber on thermal performance.

The results were confirmed using a thermal imaging camera to monitor the thermal performance over time in response to the changes in temperature (Figure 15).

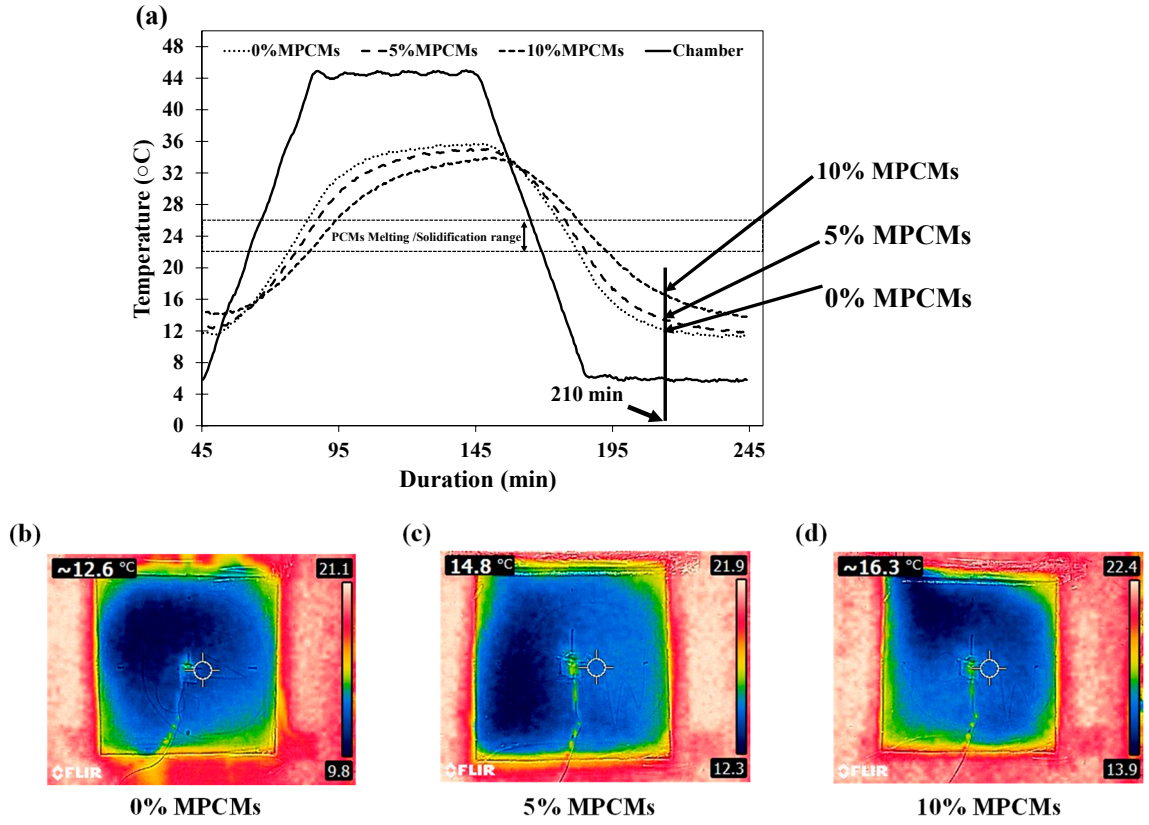

Figure 15. Monitoring the performance using thermal camera (210 min): (**a**) Temperature profile. (**b**) Thermal image for 0%MPCMs sheet. (**c**) Thermal image for 5%MPCMs sheet. (**d**) Thermal image for 10%MPCMs sheet.

4. Conclusions

The effects of microencapsulated phase change materials (MPCMs) and micro steel fibers on the workability, mechanical properties, thermal performance, and impact strength of UHPC were investigated. Based on the results presented in this paper, the following are the conclusions made from the experimental and analytical evaluation of the design mixes of MPCM-UHPC.

- Slump flow test showed that the addition of MPCMs had no significant effect on the flowability of UHPC, while the inclusion of micro steel fibers significantly decreased the flowability.
- In terms of compressive strength, adding 1.0% fiber counteracts the reduction in strength caused by the inclusion of MPCMs, while using 1.5% fiber results in higher compressive strength than the control group. On the other hand, incorporating 0.5% fiber helps to offset some of the strength loss.
- For flexural strength, adding 0.5% fiber eliminates the reduction in the strength due to MPCM incorporation, while adding 1.0% and 1.5% fiber achieved flexural strength higher than the control.
- The study analyzed the impact energy absorption of the mixtures and found that the increase in the amount of micro steel fiber or MPCMs can improve the energy dissipation capacity of concrete.
- Increasing the amount of MPCMs enhanced the thermal performance of the produced UHPC panels through the ability to absorb and release the energy during the phase change process.

Author Contributions: Conceptualization, A.M.S.; methodology, A.M.S. and M.R.; software, M.R.; validation, A.M.S. and M.R.; formal analysis, M.R.; investigation, M.R.; resources, A.M.S.; data curation, M.R.; writing—original draft preparation, M.R.; writing—review and editing, A.M.S.; visualization, M.R.; supervision, A.M.S.; project administration, A.M.S. and M.R.; funding acquisition, A.M.S. All authors have read and agreed to the published version of the manuscript.

Funding: This research was funded by Fonds Québecois de la Recherche sur la Nature et les Technologies (Nouveaux Chercheurs), Grant number 2020-NC-271140 (Holder: Ahmed M. Soliman).

Data Availability Statement: All data and results are available on Concordia library website for theses and dissertations (Advanced Search—ProQuest Dissertations & Theses Global—ProQuest).

Acknowledgments: Authors acknowledge FRQNT for providing funds for the project. Also, the authors would like to thank BCEE Concordia Machine shop for fabricating the testing equipment.

Conflicts of Interest: The authors declare no conflict of interest.

References

1. Huang, H.; Zhou, Y.; Huang, R.; Wu, H.; Sun, Y.; Huang, G.; Xu, T. Optimum insulation thicknesses and energy conservation of building thermal insulation materials in Chinese zone of humid subtropical climate. *Sustain. Cities Soc.* **2020**, *52*, 101840. [CrossRef]
2. Drissi, S.; Ling, T.-C.; Mo, K.H.; Eddhahak, A. A review of microencapsulated and composite phase change materials: Alteration of strength and thermal properties of cement-based materials. *Renew. Sustain. Energy Rev.* **2019**, *110*, 467–484. [CrossRef]
3. Saffari, M.; de Gracia, A.; Ushak, S.; Cabeza, L.F. Passive cooling of buildings with phase change materials using whole-building energy simulation tools: A review. *Renew. Sustain. Energy Rev.* **2017**, *80*, 1239–1255. [CrossRef]
4. Mahlia, T.; Saktisahdan, T.; Jannifar, A.; Hasan, M.; Matseelar, H. A review of available methods and development on energy storage; technology update. *Renew. Sustain. Energy Rev.* **2014**, *33*, 532–545. [CrossRef]
5. Salunkhe, P.B.; Shembekar, P.S. A review on effect of phase change material encapsulation on the thermal performance of a system. *Renew. Sustain. Energy Rev.* **2012**, *16*, 5603–5616. [CrossRef]
6. Cabeza, L.F.; Barreneche, C.; Martorell, I.; Miró, L.; Sari-Bey, S.; Fois, M.; Paksoy, H.O.; Sahan, N.; Weber, R.; Constantinescu, M.; et al. Unconventional experimental technologies available for phase change materials (PCM) characterization. Part 1. Thermophysical properties. *Renew. Sustain. Energy Rev.* **2015**, *43*, 1399–1414. [CrossRef]
7. Aydin, D.; Utlu, Z.; Kincay, O. Thermal performance analysis of a solar energy sourced latent heat storage. *Renew. Sustain. Energy Rev.* **2015**, *50*, 1213–1225. [CrossRef]
8. Zhou, Z.; Zhang, Z.; Zuo, J.; Huang, K.; Zhang, L. Phase change materials for solar thermal energy storage in residential buildings in cold climate. *Renew. Sustain. Energy Rev.* **2015**, *48*, 692–703. [CrossRef]
9. Solé, A.; Miró, L.; Barreneche, C.; Martorell, I.; Cabeza, L.F. Review of the T -history method to determine thermophysical properties of phase change materials (PCM). *Renew. Sustain. Energy Rev.* **2013**, *26*, 425–436. [CrossRef]
10. Li, G. Energy and exergy performance assessments for latent heat thermal energy storage systems. *Renew. Sustain. Energy Rev.* **2015**, *51*, 926–954. [CrossRef]
11. Huang, X.; Alva, G.; Jia, Y.; Fang, G. Morphological characterization and applications of phase change materials in thermal energy storage: A review. *Renew. Sustain. Energy Rev.* **2017**, *72*, 128–145. [CrossRef]
12. Cui, Y.; Xie, J.; Liu, J.; Wang, J.; Chen, S. A review on phase change material application in building. *Adv. Mech. Eng.* **2017**, *9*, 1687814017700828. [CrossRef]
13. Cabeza, L.F.; Castell, A.; Barreneche, C.; De Gracia, A.; Fernández, A.I. Materials used as PCM in thermal energy storage in buildings: A review. *Renew. Sustain. Energy Rev.* **2011**, *15*, 1675–1695. [CrossRef]
14. Akeiber, H.; Nejat, P.; Majid, M.Z.A.; Wahid, M.A.; Jomehzadeh, F.; Famileh, I.Z.; Calautit, J.K.; Hughes, B.R.; Zaki, S.A. A review on phase change material (PCM) for sustainable passive cooling in building envelopes. *Renew. Sustain. Energy Rev.* **2016**, *60*, 1470–1497. [CrossRef]
15. Johra, H.; Heiselberg, P. Influence of internal thermal mass on the indoor thermal dynamics and integration of phase change materials in furniture for building energy storage: A review. *Renew. Sustain. Energy Rev.* **2017**, *69*, 19–32. [CrossRef]
16. Kenisarin, M.; Mahkamov, K. Passive thermal control in residential buildings using phase change materials. *Renew. Sustain. Energy Rev.* **2016**, *55*, 371–398. [CrossRef]
17. Sharma, A.; Tyagi, V.V.; Chen, C.R.; Buddhi, D. Review on thermal energy storage with phase change materials and applications. *Renew. Sustain. Energy Rev.* **2009**, *13*, 318–345. [CrossRef]
18. Rao, V.V.; Parameshwaran, R.; Ram, V.V. PCM-mortar based construction materials for energy efficient buildings: A review on research trends. *Energy Build.* **2018**, *158*, 95–122. [CrossRef]
19. Memon, S.A. Phase change materials integrated in building walls: A state of the art review. *Renew. Sustain. Energy Rev.* **2014**, *31*, 870–906. [CrossRef]
20. Soares, N.; Costa, J.J.; Gaspar, A.R.; Santos, P. Review of passive PCM latent heat thermal energy storage systems towards buildings' energy efficiency. *Energy Build.* **2013**, *59*, 82–103. [CrossRef]

21. Song, M.; Niu, F.; Mao, N.; Hu, Y.; Deng, S. Review on building energy performance improvement using phase change materials. *Energy Build.* **2018**, *158*, 776–793. [CrossRef]
22. Arumugam, P.; Ramalingam, V.; Vellaichamy, P. Effective PCM, insulation, natural and/or night ventilation techniques to enhance the thermal performance of buildings located in various climates—A review. *Energy Build.* **2022**, *258*, 111840. [CrossRef]
23. Da Cunha, S.R.L.; de Aguiar, J.L.B. Phase change materials and energy efficiency of buildings: A review of knowledge. *J. Energy Storage* **2020**, *27*, 101083. [CrossRef]
24. Marani, A.; Nehdi, M.L. Integrating phase change materials in construction materials: Critical review. *Constr. Build. Mater.* **2019**, *217*, 36–49. [CrossRef]
25. Marani, A.; Zhang, L.V.; Nehdi, M.L. Multiphysics study on cement-based composites incorporating green biobased shape-stabilized phase change materials for thermal energy storage. *J. Clean. Prod.* **2022**, *372*, 133826. [CrossRef]
26. Balapour, M.; Mutua, A.W.; Farnam, Y. Evaluating the thermal efficiency of microencapsulated phase change materials for thermal energy storage in cementitious composites. *Cem. Concr. Compos.* **2020**, *116*, 103891. [CrossRef]
27. Tian, Y.; Lai, Y.; Qin, Z.; Pei, W. Numerical investigation on the thermal control performance and freeze-thaw resistance of a composite concrete pier with microencapsulated phase change materials. *Sol. Energy* **2021**, *231*, 970–984. [CrossRef]
28. Sivanathan, A.; Dou, Q.; Wang, Y.; Li, Y.; Corker, J.; Zhou, Y.; Fan, M. Phase change materials for building construction: An overview of nano-/micro-encapsulation. *Nanotechnol. Rev.* **2020**, *9*, 896–921. [CrossRef]
29. Cui, H.; Tang, W.; Qin, Q.; Xing, F.; Liao, W.; Wen, H. Development of structural-functional integrated energy storage concrete with innovative macro-encapsulated PCM by hollow steel ball. *Appl. Energy* **2017**, *185*, 107–118. [CrossRef]
30. Hunger, M.; Entrop, A.; Mandilaras, I.; Brouwers, H.; Founti, M. The behavior of self-compacting concrete containing micro-encapsulated Phase Change Materials. *Cem. Concr. Compos.* **2009**, *31*, 731–743. [CrossRef]
31. Kuznik, F.; David, D.; Johannes, K.; Roux, J.-J. A review on phase change materials integrated in building walls. *Renew. Sustain. Energy Rev.* **2011**, *15*, 379–391. [CrossRef]
32. Aguayo, M.; Das, S.; Maroli, A.; Kabay, N.; Mertens, J.C.; Rajan, S.D.; Sant, G.; Chawla, N.; Neithalath, N. The influence of microencapsulated phase change material (PCM) characteristics on the microstructure and strength of cementitious composites: Experiments and finite element simulations. *Cem. Concr. Compos.* **2016**, *73*, 29–41. [CrossRef]
33. Eddhahak, A.; Drissi, S.; Colin, J.; Caré, S.; Neji, J. Effect of phase change materials on the hydration reaction and kinetic of PCM-mortars. *J. Therm. Anal. Calorim.* **2014**, *117*, 537–545. [CrossRef]
34. Lecompte, T.; Le Bideau, P.; Glouannec, P.; Nortershauser, D.; Le Masson, S. Mechanical and thermo-physical behaviour of concretes and mortars containing phase change material. *Energy Build.* **2015**, *94*, 52–60. [CrossRef]
35. Meshgin, P.; Xi, Y. Effect of phase-change materials on properties of concrete. *ACI Mater. J.* **2012**, *109*, 71.
36. Pomianowski, M.; Heiselberg, P.; Jensen, R.L.; Cheng, R.; Zhang, Y. A new experimental method to determine specific heat capacity of inhomogeneous concrete material with incorporated microencapsulated-PCM. *Cem. Concr. Res.* **2014**, *55*, 22–34. [CrossRef]
37. Amran, M.; Huang, S.-S.; Onaizi, A.M.; Makul, N.; Abdelgader, H.S.; Ozbakkaloglu, T. Recent trends in ultra-high performance concrete (UHPC): Current status, challenges, and future prospects. *Constr. Build. Mater.* **2022**, *352*, 129029. [CrossRef]
38. Hakeem, I.Y.; Althoey, F.; Hosen, A. Mechanical and durability performance of ultra-high-performance concrete incorporating SCMs. *Constr. Build. Mater.* **2022**, *359*, 129430. [CrossRef]
39. Wang, Y.; Wang, J.; Wu, Y.; Li, Y.; He, X.; Su, Y.; Strnadel, B. Preparation of sustainable ultra-high performance concrete (UHPC) with ultra-fine glass powder as multi-dimensional substitute material. *Constr. Build. Mater.* **2023**, *401*, 132857. [CrossRef]
40. Yazıcı, H.; Yardımcı, M.Y.; Aydın, S.; Karabulut, A.Ş. Mechanical properties of reactive powder concrete containing mineral admixtures under different curing regimes. *Constr. Build. Mater.* **2009**, *23*, 1223–1231. [CrossRef]
41. Shi, C.; Wu, Z.; Xiao, J.; Wang, D.; Huang, Z.; Fang, Z. A review on ultra high performance concrete: Part I. Raw materials and mixture design. *Constr. Build. Mater.* **2015**, *101*, 741–751. [CrossRef]
42. Ghafari, E.; Ghahari, S.A.; Costa, H.; Júlio, E.; Portugal, A.; Durães, L. Effect of supplementary cementitious materials on autogenous shrinkage of ultra-high performance concrete. *Constr. Build. Mater.* **2016**, *127*, 43–48. [CrossRef]
43. Xue, C.; Yu, M.; Xu, H.; Xu, L.; Saafi, M.; Ye, J. Experimental study on thermal performance of ultra-high performance concrete with coarse aggregates at high temperature. *Constr. Build. Mater.* **2022**, *314*, 125585. [CrossRef]
44. Ren, M.; Wen, X.; Gao, X.; Liu, Y. Thermal and mechanical properties of ultra-high performance concrete incorporated with microencapsulated phase change material. *Constr. Build. Mater.* **2021**, *273*, 121714. [CrossRef]
45. *CSA A3000-13*; Cementitious Materials Compendium. CSA Group: Mississauga, ON, Canada, 2013.
46. Standard Specification for Silica Fume Used in Cementitious Mixtures. Available online: https://www.astm.org/c1240-20.html (accessed on 19 February 2023).
47. Standard Specification for Coal Fly Ash and Raw or Calcined Natural Pozzolan for Use in Concrete. Available online: https://www.astm.org/c0618-22.html (accessed on 5 April 2023).
48. Rahman, O.A.; Al-Shdaifat, M.; Almakhadmeh, M.; Soliman, A. Phase change materials sheets for energy-efficient heat curing process: A potential idea and performance evaluation. *Constr. Build. Mater.* **2022**, *353*, 129102. [CrossRef]
49. Standard Test Method for Flow of Hydraulic Cement Mortar. Available online: https://www.astm.org/c1437-15.html (accessed on 19 February 2023).

50. Standard Test Method for Compressive Strength of Hydraulic Cement Mortars (Using 2-in. or [50 mm] Cube Specimens). Available online: https://www.astm.org/c0109_c0109m-21.html (accessed on 19 February 2023).
51. Standard Test Method for Flexural Strength of Hydraulic-Cement Mortars. Available online: https://www.astm.org/c0348-21.html (accessed on 19 February 2023).
52. Yu, R.; van Beers, L.; Spiesz, P.; Brouwers, H.J.H. Impact resistance of a sustainable Ultra-High Performance Fibre Reinforced Concrete (UHPFRC) under pendulum impact loadings. *Constr. Build. Mater.* **2016**, *107*, 203–215. [CrossRef]
53. Yu, R.; Spiesz, P.; Brouwers, H.J.H. Mix design and properties assessment of Ultra-High Performance Fibre Reinforced Concrete (UHPFRC). *Cem. Concr. Res.* **2014**, *56*, 29–39. [CrossRef]
54. Gao, X.M. *Effect of Steel Fiber on the Performance Of Ultra-High Performance Concrete*; Hunan University: Changsha, China, 2013.
55. Yunsheng, Z.; Wei, S.; Sifeng, L.; Chujie, J.; Jianzhong, L. Preparation of C200 green reactive powder concrete and its static–dynamic behaviors. *Cem. Concr. Compos.* **2008**, *30*, 831–838. [CrossRef]
56. Banthia, N.; Trottier, J.-F. Concrete reinforced with deformed steel fibres. Part II: Toughness characterization. *ACI Mater. J.* **1995**, *92*, 146–154.
57. Essid, N.; Loulizi, A.; Neji, J. Compressive strength and hygric properties of concretes incorporating microencapsulated phase change material. *Constr. Build. Mater.* **2019**, *222*, 254–262. [CrossRef]
58. Pilehvar, S.; Szczotok, A.M.; Rodríguez, J.F.; Valentini, L.; Lanzón, M.; Pamies, R.; Kjøniksen, A.-L. Effect of freeze-thaw cycles on the mechanical behavior of geopolymer concrete and Portland cement concrete containing micro-encapsulated phase change materials. *Constr. Build. Mater.* **2019**, *200*, 94–103. [CrossRef]
59. Gürbüz, E.; Erdem, S. Development and thermo-mechanical analysis of high-performance hybrid fibre engineered cementitious composites with microencapsulated phase change materials. *Constr. Build. Mater.* **2020**, *263*, 120139. [CrossRef]
60. Wu, Z.; Shi, C.; Khayat, K.H. Investigation of mechanical properties and shrinkage of ultra-high performance concrete: Influence of steel fiber content and shape. *Compos. Part B Eng.* **2019**, *174*, 107021. [CrossRef]
61. Barnett, S.J.; Lataste, J.-F.; Parry, T.; Millard, S.G.; Soutsos, M.N. Assessment of fibre orientation in ultra high performance fibre reinforced concrete and its effect on flexural strength. *Mater. Struct.* **2010**, *43*, 1009–1023. [CrossRef]
62. Yoo, D.-Y.; Shin, H.-O.; Yang, J.-M.; Yoon, Y.-S. Material and bond properties of ultra high performance fiber reinforced concrete with micro steel fibers. *Compos. Part B Eng.* **2014**, *58*, 122–133. [CrossRef]
63. Kang, S.-T.; Kim, J.-K. The relation between fiber orientation and tensile behavior in an Ultra High Performance Fiber Reinforced Cementitious Composites (UHPFRCC). *Cem. Concr. Res.* **2011**, *41*, 1001–1014. [CrossRef]
64. Fernandes, F.; Manari, S.; Aguayo, M.; Santos, K.; Oey, T.; Wei, Z.; Falzone, G.; Neithalath, N.; Sant, G. On the feasibility of using phase change materials (PCMs) to mitigate thermal cracking in cementitious materials. *Cem. Concr. Compos.* **2014**, *51*, 14–26. [CrossRef]
65. Wang, H.; Wang, L. Experimental study on static and dynamic mechanical properties of steel fiber reinforced lightweight aggregate concrete. *Constr. Build. Mater.* **2013**, *38*, 1146–1151. [CrossRef]
66. Song, H.W.; Wang, H.T. Statistical Evaluation for Impact Resistance of Steel Fiber Reinforced Lightweight Aggregate Concrete. *Adv. Mater. Res.* **2011**, *250–253*, 609–613. [CrossRef]
67. Erdem, S.; Gürbüz, E. Influence of microencapsulated phase change materials on the flexural behavior and micromechanical impact damage of hybrid fibre reinforced engineered cementitious composites. *Compos. Part B Eng.* **2019**, *166*, 633–644. [CrossRef]
68. Dorf, V.; Krasnovskiy, R.; Kapustin, D.; Sultygova, P.; Umnyakova, N. Influence of fiber content on the conductivity of steel fiber-reinforced concrete. *Spec. Publ.* **2018**, *326*, 62.1–62.8.
69. Shubin, I.L.; Dorf, V.A.; Krasnovskij, R.O.; Kapustin, D.E.; Sultygova, P.S. Study of the Thermophysical Characteristics of Steel Fiber Reinforced Concrete. *Mater. Sci. Forum* **2020**, *992*, 41–47. [CrossRef]
70. Cui, H.; Zou, J.; Gong, Z.; Zheng, D.; Bao, X.; Chen, X. Study on the thermal and mechanical properties of steel fibre reinforced PCM-HSB concrete for high performance in energy piles. *Constr. Build. Mater.* **2022**, *350*, 128822. [CrossRef]
71. Liang, X.; Wu, C. Investigation on thermal conductivity of steel fiber reinforced concrete using mesoscale modeling. *Int. J. Thermophys.* **2018**, *39*, 142. [CrossRef]
72. Nagy, B.; Nehme, S.G.; Szagri, D. Thermal Properties and Modeling of Fiber Reinforced Concretes. *Energy Procedia* **2015**, *78*, 2742–2747. [CrossRef]